
Article:
Renzoni, A.M., Kelley, W.L., Rosato, R.R. et al. (9 more authors) (2017) Molecular bases determining daptomycin resistance-mediated re-sensitization to β-lactams ("see-saw effect") in MRSA. Antimicrobial Agents and Chemotherapy, 61 (1). e01634-16. ISSN 0066-4804

https://doi.org/10.1128/AAC.01634-16

Molecular bases determining daptomycin resistance-mediated re-sensitization to β-lactams ("see-saw effect") in MRSA

Adriana M. Renzoni[a], William L. Kelley[b], Roberto R. Rosato[c], Maria P. Martinez[c], Melanie Roch[c], Maryam Fatouraei[c], Daniel P. Haeusser[d], William Margolin[d], Samuel Fenn[e], Robert D. Turner[e], Simon J. Foster[e] and Adriana E. Rosato[c*]

[a]Hopitaux Universitaires de Genève, Service of Infectious Diseases, Geneva, Switzerland

[b]University of Geneva Medical School, Department of Microbiology and Molecular Medicine, Geneva, Switzerland

[c]Department of Pathology and Genomic Medicine, Center for Molecular and Translational Human Infectious Diseases Research, Houston Methodist Research Institute, Houston, TX

[d]Department of Microbiology and Molecular Genetics, McGovern Medical School, University of Texas, Houston, TX

[e]Krebs Institute, University of Sheffield, Firth Court, Western Bank, Sheffield, United Kingdom

[*]Corresponding author:

Houston Methodist Research Institute, 6670 Bertner Ave., Room R6-113, Houston, TX 77030

Phone: 713-441-4369; Fax: 713-441-2895

E-mail: aerosato@HoustonMethodist.org

Short title: Daptomycin/β-lactams/PrsA and MRSA

Keywords: MRSA, daptomycin, see-saw effect, β-lactams, PrsA

ABSTRACT

Antimicrobial resistance is recognized as one of the principal threats to public health worldwide, yet the problem is increasing. Methicillin–resistant *Staphylococcus aureus* (MRSA) are among the most difficult to treat in clinical settings due to the resistance to nearly all available antibiotics. The cyclic anionic lipopeptide antibiotic Daptomycin (DAP) is the clinical mainstay of anti-MRSA therapy. Decreased susceptibility to DAP (DAPR) reported in MRSA is frequently accompanied with a paradoxical decrease in β-lactam resistance, a process known as the "see-saw" effect. Despite the observed discordance in resistance phenotypes, the combination of DAP/β-lactams has been proven clinically effective for the prevention and treatment of infections due to DAPR-MRSA strains. However, the mechanisms underlying the interactions between DAP and β-lactams are largely unknown. Herein, we studied the role of DAP-induced mutated *mprF* in β-lactam sensitization and its involvement in the effective killing by the DAP/OXA combination. DAP/OXA-mediated effects resulted in cell-wall perturbations including changes in peptidoglycan (PG) insertion, penicillin-binding protein 2 (PBP2) delocalization and reduced membrane amounts of penicillin-binding protein 2a (PBP2a) contents despite increased transcription of *mecA* through *mec* regulatory elements. We have found that the VraSR sensor-regulator is a key component of DAP resistance, triggering mutated *mprF*-mediated cell membrane (CM) modifications and resulting in impairment of PrsA location and chaperone functions, both essentials for PBP2a maturation, the key determinant of β-lactam resistance. These observations provide first time evidence that synergistic effects between DAP and β-lactams involve PrsA post-transcriptional regulation of CM-associated PBP2a.

INTRODUCTION

S. aureus has a proclivity for developing multidrug resistance (e.g., methicillin-resistant *S. aureus*, MRSA) and infections with this pathogen result in enhanced attributable mortality (33). Since its FDA approval in 2003, the cyclic anionic lipopeptide antibiotic daptomycin (DAP) produced by *Streptomyces roseosporus* (3), has become the clinical mainstay of anti-MRSA therapy due to its potent staphylocidal activity (1). The mechanism of action of DAP involves the disruption of cytoplasmic membrane (CM) function leading to its depolarization and causing cell death (2). However, there have been a number of reports in which initially DAP-susceptible (DAPS) MRSA strains developed DAP resistant (DAPR) phenotypes during clinical treatment failures (4,28). DAPR strains obtained from therapeutic failure are associated with a number of gene mutations linked with DAP resistance, including those in CM associated genes (e.g. *mprF*) and cell wall (CW) (e.g., the two-component system YycFG), and others as mutations in RNA polymerase subunits RpoB/C (16). However, the most clinically significant and relevant changes are those associated with mutations in *mprF* (4,28). In previous studies, we demonstrated by using sets of isogenic DAPS and DAPR strains that, in addition to *mprF,* resistance to DAP involved the upregulation of genes involved in CW synthesis and turnover, including the two-component regulator and CW stress stimulon *vraSR* (28). Together, these observations led us to postulate that both CM and CW components contribute to decreased susceptibility to DAP.

Interestingly, we and others have observed both *in vitro* (29,38,49) and *in vivo* (13,29,30) that DAP resistance sensitizes MRSA to β-lactams, notably oxacillin, a process known as a "see-saw" effect (29). Indeed, we have demonstrated that combinations of DAP with OXA (*in-vitro*) or nafcillin (NAF) (*in-vivo*), as well as other β-lactams such as cefotaxime (CTX), which targets PBP2, and carbapenems, such as imipenem (IPM) that target PBP1, displayed strong synergistic interactions

against DAP resistant MRSA (29). Although the DAP/β-lactam combination is extensively used in clinical settings for the treatment of MRSA infections associated with decreased susceptibility to DAP (29), the mechanistic bases of the "see-saw" effect remain to be elucidated.

The PrsA protein is required for resistance to oxacillin as well as glycopeptide antibiotics in *S. aureus* (21,22). In Gram-positive bacteria such as *Bacillus subtilis* and *Listeria monocytogenes*, PrsA is a membrane-anchored protein that catalyzes the post-translocational folding of exported proteins, and is essential for their stability as they cross the bacterial cell membrane-cell wall interface (34,41). In *B. subtilis*, PrsA is required for folding of PBPs and lateral cell wall biosynthesis; in the absence of PrsA, four PBPs (PBP2a, PBP2b, PBP3 and PBP4) become unstable (8). Additionally, in *L. monocytogenes*, PrsA2 contributes to bacterial pathogenesis and virulence (10). Expression of *prsA* is induced upon encountering cell wall active antibiotics and induction is dependent upon the activity of VraSR, the cell wall stress two-component system (22). Importantly, the same authors reported that cells were more susceptible to oxacillin in the absence of PrsA, suggesting that PrsA may be involved in oxacillin resistance in concert with VraSR, PBP2 and PBP2a (22). Recent PrsA structure and function analyses revealed that PrsA modulates PBP2a protein levels independent of the SCC*mec* background strains (21). Regulation of PBP2a expression at the transcriptional level involves *mecI*, *mecR*, and *blaRZ,* which may vary in SCC*mec* types, but less is known about the post-transcriptional maturation and proper localization of PBP2A.

In the present study, we demonstrate that DAPR-mediated *mprF* mutations result in significant changes in cell wall synthesis by influencing the function of PrsA, which correlates with reduced amounts of β-lactam-induced PBP2a. This work provides evidence that MprF and PrsA are important for the sensitization to β-lactams during DAP resistance in MRSA (see-saw effect), and contributes new insights into the mechanisms associated to this effect.

MATERIALS AND METHODS

Bacterial strains, plasmids and antibiotics. All clinical strains used in this study are listed in Table 1. Trypticase Soy Agar with 5% sheep blood (BBL, Sparks, MD) was used for subculture and maintenance of *S. aureus*. *Staphylococcus aureus* and *E.coli* were grown in Mueller-Hinton Broth (MHB). Standard reference antibiotics, tetracycline (TET, 3ug/ml), chloramphenicol (CM, 10ug/ml), oxacillin (OXA) range 0.5 to 10 µg/ml) were obtained from Sigma, St. Louis, MO; United States Biochemicals, Cleveland, OH Daptomycin (DAP) was provided by Cubist Pharmaceuticals/Merck (Lexington, MA). DAP and OXA were used at concentrations adjusted based on strains MICs in parental and genetic mutants. Calcium was added at concentration of 50 mg/L for DAP. Antimicrobial susceptibility to OXA was determined according to the guidelines of the Clinical and Laboratory Standards Institute (32). DAP MICs were determined by Etest (AB Biodisk, Solna, Sweden).

Membrane protein extraction. For the isolation of membrane proteins, strains were grown in MHB until mid-exponential phase and pellets were resuspended in 600 µl of PBS. Bacterial cells were disrupted by adding glass beads and using a FastPrep cell disrupter (MP Biomedicals, Santa Ana, CA) and the lysate was centrifuged at 8,000 g for 10 min at 4°C. The supernatant fraction was centrifuged for additional 5 min at 8,000 g at 4°C to remove beads and then the supernatant was transferred to ultracentrifuge tubes and centrifuged at 45,000 rpm in a Thermo Sorvall WX ULtra Series WX80 (Thermo Scientific, Waltham, MA) for 1 h at 4°C. The membrane pellet was resuspended in PBS and total membrane proteins were quantified by Bradford protein assay (Thermo Fisher) and stored at -80°C.

Secreted protein preparation. Bacteria were grown in MHB until OD_{600} aprox. 0.3. Then samples were centrifuged for 10 min at 4,000 rpm and the supernatant was passed through 0.22 µm

membrane filters (Millex). Samples were normalized by volume adjustment to equal sample OD and 20 µg of carbonic anhydrase (Sigma) were added as an internal spike control as described (Andrey et al., 2015). Samples were concentrated in Amicon 10000MWCO centrifugal filters (Millipore) to a final volume of 40 µl.

Western blotting. Proteins (15 µg) were separated on 4-12% Bis-Tris gels and blot transferred onto pure nitrocellulose blotting membranes (PALL Life Science). Membranes were blocked using 5% low-fat milk in PBS. PBP2A was probed with monoclonal anti-PBP2A antibody (Slidex MRSA Detection kit, BioMerieux, France) at a 1/2000 dilution followed by incubation with a secondary alkaline phosphatase-labeled goat anti-rabbit lgG (H+L) antibody at a 1/5000 dilution. Labelled protein signal was detected using a SRX/101A Film Processor (Konica Minolta).

DNA manipulation and sequencing. Chromosomal DNA was prepared by using a Qiagen genomic DNA preparation kit (Qiagen, Inc. Valencia, CA) according to the manufacturer's directions. Sequencing of all PCR amplification products was performed at the Nucleic Acid Research Facility at GENEWIZ (South Plainfield, NJ). Sequence analysis of *mprF* in wild type strains and mutants was performed by using *mprF* primers as previously described (28). Consensus sequences were assembled from both orientations with Lasergene 12 software (DNASTAR, Madison, WI). *S. aureus* N315 (accession # BA000018) was used as a reference sequence control.

RNA extraction and RNA-Seq. Total RNA was extracted using an RNeasy isolation kit (Qiagen). The concentration and integrity of RNA samples was assessed by A_{260}/A_{280} spectrophotometry and gel electrophoresis. RNA samples were cleaned and treated with DNase following the manufacturer's recommendations to avoid potential DNA contamination. RNA was prepared from CB1634 cells collected at exponential phase of growth at the different conditions in absence and presence of DAP, OXA and DAP/OXA. The genome-wide transcript sequencing libraries were

prepared according the manufacturer's instructions (ScriptSeq, EpiCentre) and sequenced on a MiSeq instrument (Illumina). Differential gene expression was determined by CLC Genomic Workbench and Lasergene software; differences >1.5 fold and P<0.05 after applying Bonferroni correction for multiple comparisons were considered significant.

Analysis of gene expression by RT-PCR. Real-time reverse transcription-PCR analysis for RNA samples were done using a SensiMix SYBR One/Step kit (Qantace/Bioline, Taunton, MA) according to the manufacturer's protocol. Gene expression was compared respect of a sample considered the reference (value = 1) using $\log_2$-($\Delta\Delta C_T$). The change (n-fold) in the transcript level was calculated using the following equations: $\Delta C_T = C_{T(\text{test DNA})} - C_{T(\text{reference cDNA})}$, $\Delta\Delta C_T = \Delta C_{T(\text{target gene})} - \Delta C_{T(16\text{SrRNA})}$ and ratio $=2^{-\Delta\Delta C_T}$. The quantity of cDNA for each experimental gene was normalized to the quantity of 16S cDNA in each sample. Oligonucleotide primers are shown in Table 1.

Microscopy, labelling and imaging of DAPS and DAPR cells. Parental DAPS; CB1631 and resistant DAPR; CB1634 strains were grown in TSB in absence and presence of DAP (0.25 and 1µg/ml, respectively) at 37°C to exponential phase, labelled for 5 min with either HADA (stains nascent peptidoglycan insertion), FM1-43FX (stains the cell membrane), DAPI (stains DNA) or vancomycin (stains nascent D-Alanyl-D-Alanine incorporation into CW) (Sigma) mixed with a BODIPY FL conjugate of vancomycin (Van-FL, Molecular Probes) to a final concentration of 0.8 µg/mL. Images were obtained with a Nikon inverted epifluorescence microscope. For localization studies of PBP2, the corresponding gene *pbpB* was expressed as an N-terminal GFP fusion protein in CB1634. Genomic DNA was PCR amplified using Phusion DNA polymerase and the primers pbp2-0F (DPH407) and pbp2-R (DPH408) (Table 1). PCR fragments were digested with NotI and BamHI and ligated into a cleaved pEA18 vector, in frame with gfp (originally cloned from pDSW207) to generate pDH177 in *E. coli* AG111 competent cells. The *gfp-pbpB* fragment, including the *B. subtilis spoVG* ribosome binding site sequence of pEA18, was subcloned from pDH177 by digestion

with HindIII and BamHI and ligated into cleaved pCL15 vector to generate pDH178. pDH178 was initially cloned into *E. coli* AG1111 (Promega Wizard), and transformed into *S. aureus* RN4220 by electroporation. The plasmid was then transduced from RN4220 into *S. aureus* CB1634 using phage 80α. CB1634 cells containing the *gfp-pbpB* gene in pDH178 were induced with IPTG in the presence of OXA, DAP, or DAP/OXA to localize PBP2a during DAP/OXA synergistic effects. Cells were fixed in 2.8% formaldehyde (FA) and 0.04% glutaraldehyde (GA) in growth medium for 15 min at room temperature. The cells were collected at 8000g for 5 min, washed once in PBS, treated with vectashield anti-fade reagent and visualized by fluorescence microscopy with an Olympus BX60 epifluorescence microscope containing a 100x oil immersion objective (N.A. 1.4). Images were captured with a Hamamatsu Orca charge-coupled device camera using HCImage software.

Labeling of PBPs with bocillin. Bocillin labelling of 100 µg of membrane proteins was performed with 100 µM bocillin-FL (Molecular Probes) incubated for 30 min at 35°C. The reaction was stopped by adding 4xSDS-PAGE sample buffer. Labelled membrane protein concentrations were determined by Bradford protein assay and 15 µg were loaded on a 10% Bis-Tris gel and detected using a ProteinSimple Imager-FluorChem E system (GE Healthcare).

Peptidoglycan purification and analysis. Exponentially growing cells (OD_{600} 0.5) grown on MHB untreated and treated with OXA, DAP and DAP/OXA were boiled in 4% Sodium dodecyl sulfate (SDS) and deproteinized by treatment with pronase and trypsin, then treated with 48% hydrofluoric acid (HF) at 4°C for 16hs, washed several times with 0.25M Tris-HCl and water before lyophilization. Purified peptidoglycan was digested with 25 µg/ml of mutanolysin (Sigma). The soluble muropeptides were reduced with sodium borohydride. The reaction was stopped by the addition of phosphoric acid and the supernatant containing peptidoglycan was analyzed in a LC-20AB HPLC equipped with a SPD-20A UV detector (Shimadzu). The separation of muropeptides was performed in a Jupiter Proteo column (C18, 250 x 4.6 mm, 4µm, 90A) (Phenomenex). 20 µl of

sample were eluted at 0.5 ml/min for 5 minutes with 95% A (100 mM sodium phosphate buffer pH 3.0 containing 0.00025% sodium azide) and 5% B (methanol) and then B was increased up to 30 % at 120 min as previously described. (18) Detection was performed at 206 nm and peaks were identified by comparison with the elution profile for peptidoglycan from COL strain previously reported (12).

Statistical analyses. Statistical tests were performed using SPSS v17.0 for Windows (SPSS Inc., Chicago, IL, USA). The survival data were plotted using the Kaplan–Meier methods.

RESULTS

Daptomycin-induced cytoplasmic membrane and cell wall changes. Despite considerable evidence pointing to the action of DAP on the CM, the CW has also been suspected to be an important target as recently shown in *B. subtilis* (17,36). We used fluorescence microscopy to visualize the effects of DAP on both CM and CW functions. When DAPS CB1631 cells were treated with DAP, they displayed significant morphological changes at the CM level (Fig. 1A, FM1-43X staining, upper panels), including shape abnormalities and size heterogeneity compared with untreated control cells (No DAP). All the cells contained DNA as judged by DAPI staining (not shown), indicating that DAP did not cause significant alterations to the nucleoid.

This observation was corroborated by analysis of the pattern of nascent peptidoglycan (PG) insertion using the fluorescent D-amino acid derivative HADA (HCC-amino-D-alanine). Exposure of DAPS CB1631 to DAP induced the delocalization of PG insertion (Fig.1A, lower panels), suggesting that PBPs were displaced from the division septum, where CW synthesis normally takes place. Importantly, none of the changes described in DAPS CB1631 were observed in the DAPR CB1634

counterpart (Fig.1B, right panels). These observations are in agreement with the hypothesis that DAP induces dramatic effects on both the CM and CW in *S. aureus*.

Effects on cell wall rearrangements during exposure to a combination of DAP and β-lactams. We previously observed that DAP-mediated sensitization to β-lactams occurred with those that preferentially target PBP1 or PBP2, including NAF (PBP1, PBP2), IPM (PBP1) and CTX (PBP2), whereas no changes were observed with β-lactams targeting PBP4 such as cefoxitin (FOX) or PBP3 such as cefaclor (CEC) (6,7,29). Similar effects were observed in other *in vitro*-selected DAPR mutants obtained from DAPS CB1631 (DAPR-CB1631) and CB5011 (DAPR-CB5011) (29). Collectively, these observations suggest that the see-saw effect involves CW modifications.

To address this in more detail, we stained cells with BodipyFL-VAN, which has been used extensively to detect the localization of newly synthesized peptidoglycan in Gram-positive bacteria (47,48). DAPR CB1634 cells were grown without/with DAP/OXA combination followed by BodipyFL-VAN staining (10 min) and detection by fluorescence microscopy (Fig. 2). In the untreated control BodipyFL-VAN intensely stained the complete equatorial cell septa and faintly the side-walls; in contrast, cells grown in the presence of DAP/OXA showed mostly delocalized BodipyFL-VAN staining (Fig. 2A). These results are consistent with the delocalized peptidoglycan insertion patterns by HADA staining (Fig. 1), and suggest that co-administration of DAP with β-lactams causes dramatic local effects on the CW in DAPR cells similar to those observed in DAPS cells (CB1631) such as displacement of PBPs from the septum). In fact, studies of the labeling of newly synthesized CW with fluorescein-conjugated VAN in *S. aureus* have suggested that most CW synthesis is confined to the division septum, where both PBP1 and PBP2 are localized (35).

To investigate further the hypothesis that the combined CW effects of DAP and β-lactams contribute to the delocalization of PBPs, particularly PBP1 and PBP2, we generated a CB1634-derivative strain

231 expressing an IPTG-regulated PBP2-GFP fusion protein. The CB1634-*PBP2-GFP* strain, untreated
232 cells showed that PBP2-GFP protein clearly localized to the equatorial cell septa (Fig. 2B). In contrast,
233 exposure to a DAP/OXA combination resulted in diffused and delocalized distribution of PBP2-GFP,
234 in agreement with the results in Fig. 2A. Similar observations were made by using the same approach
235 with a PBP1-GFP fusion protein (data not shown). We next wanted to determine the activity of PBPs
236 by measuring their binding affinity to a fluorescent β-lactam, Bocillin FL. The DAPR CB1634 strain
237 was exposed to DAP (1µg/ml), OXA (0.5µg/ml) and DAP/OXA (1µg/ml/0.5µg/ml, respectively),
238 and PBPs separated by SDS-PAGE were analyzed for their ability to bind Bocillin FL. As shown in
239 Fig. 3, DAPR CB1634 cells treated with DAP/OXA and subsequently labelled with bocillin
240 displayed a decreased levels of PBP1, PBP2 and PBP3, whereas no changes were observed with
241 either DAP and/or OXA alone. However, since we have previously shown that inhibition of PBP3 by
242 CEC did not result in see-saw effect when combined with DAP (29), the present results may indicate
243 that PBP1 and PBP2 have a relevant role in the DAP-associated see-saw effect and restoration of
244 susceptibility to β-lactams in (MRSA) DAPR strains.

245

246 **Sensitization to β-lactams during DAP resistance is associated with decreased production of**
247 **PBP2a.** β-lactam resistance in MRSA involves the horizontal acquisition of the *mecA* gene, which
248 encodes PBP2a, a PBP with low affinity for β-lactams that can mediate cell wall assembly when the
249 normal staphylococcal PBPs (PBP1 to 4) are inactivated by these agents (35). To determine a
250 potential role for PBP2a in the DAP-mediated see-saw effect observed in DAPR strains, PBP2a
251 protein expression levels were analyzed by western blotting using cell membrane protein extracts
252 prepared from CB1634 treated with OXA, DAP and the DAP/OXA combination. Compared to
253 untreated control cells, no PBP2a induction was observed with DAP, while as expected, the levels of

254 PBP2a increased significantly after exposure to OXA (Fig. 4A). Importantly, in DAP/OXA-treated
255 CB1634 cells there was a marked reduction in PBP2a levels when compared to OXA induction.
256 Analysis of OD_{600}-normalized extracellular extracts showed increased amounts of extracellular
257 PBP2a in the corresponding CB1634 treated with DAP/OXA strain while no extracellular PBP2a
258 was detected in extracts from collected from the control untreated sample (Fig. 4A). A slight
259 increase on the extracellular amounts of PBP2a was also observed in extracts from OXA-treated
260 cells, consistent with increasing amounts of cell membrane-associated protein. These results strongly
261 suggest that PBP2a localization to the CM is altered, which in turn would be associated with the
262 DAPR phenotype mediated see-saw effect.

263 To determine whether reduction of PBP2a levels observed with the DAP/OXA combination was
264 linked to alterations in *mecA* transcriptional regulation, we evaluated *mecA* mRNA levels in the
265 absence and presence of DAP, OXA and DAP/OXA by real-time RT-PCR analysis. We found that
266 *mecA* transcription in the CB1634 strain displayed significant induction by OXA alone, an effect that
267 was further enhanced in the case of OXA/DAP (Fig. 4B); a modest induction was also observed
268 upon exposure to DAP. These results do not correlate with the changes in CM-associated PBP2a
269 protein levels subject to the various drug combinations, and thus cannot be attributed solely to
270 changes in the transcription of the *mecA* gene. Furthermore, the results strongly suggest that these
271 alterations during the see-saw effect may critically interfere with the normal synthesis/function of
272 the CW.

273 We next wanted to establish whether DAP-induced mutations in *mprF,* which potentially are
274 associated with changes in the CM, may play a role in PBP2a and CW changes observed during the
275 see-saw effect. To address this, we analyzed PBP2a protein levels using membrane protein extracts
276 from DAPR-CB1634, CB1634Δ*mprF*, and CB1634Δ*mprF* complemented either with WT-*mprF* or a
277 previously isolated *mprF* mutant (*mprFL826F*) that is associated with decreased susceptibility to

DAP (28). As depicted in Fig. 4C, cellular levels of membrane-associated PBP2a were sharply increased by exposure to OXA in all strains compared to either the corresponding untreated controls or DAP-treated cells. Importantly, the strong reduction of PBP2a levels in the parental CB1634 strain exposed to DAP/OXA (Fig. 4A) was not observed in the CB1634Δ*mprF* strain MAR17 (Fig. 4C). Interestingly, complementation of MAR17 with WT-*mprF* (MAR18 strain) resulted in the same PBP2a profile detected in MAR17, indicating that there were no differences in the amount of CM-associated protein between OXA- and DAP/OXA-treated cells. However, PBP2a levels were significantly reduced in CB1634Δ*mprF* complemented with *mprFL826F* (strain MAR19), following the same pattern observed in the parental CB1634 displaying the see-saw effect. These results indicate that DAP-mediated changes in *mprF* and/or the CM associated with the DAPR phenotype alter the membrane levels of PBP2a and thereby may interfere with the normal synthesis/function of the CW.

Functional role of *mprF* mutations on peptidoglycan cross-linking and DAP availability during DAPR and the see-saw effect. Given the effects of altered MprF on PBP2a levels, we next wanted to determine the influence of *mprF* mutations on the DAP-mediated "see-saw" effect. Phenotypic analysis comparing DAPR CB1634 *vs.* its CB1634Δ*mprF* counterpart showed that inactivation of *mprF* led to increased susceptibility to DAP (MIC DAP: 4 µl/ml vs. 0.25 µl/ml, respectively), and increased resistance to OXA (MIC OXA: 0.5 µl/ml vs. 32 µl/ml, respectively; Table 2). Importantly, complementation of CB1634Δ*mprF* with WT *mpr*F did not revert the phenotype (DAP or OXA MIC: 0.75 µg/ml *vs.* 32 µg/ml, respectively). In contrast, complementation with *mprF*L826F restored the resistance to DAP (MIC = 3 µg/ml) and decreased resistance to OXA (MIC = 1 µg/ml), re-establishing the DAP-mediated "see-saw" effect (Table 2). Similar results were observed with the DAPS/R pair CB5011/CB5012-(*mprFL826F*) (data not shown).

We next determined the impact of *mprF* mutations and the implications of altered levels of PBP2a on the CW during the DAP-mediated see-saw effect. The muropeptide composition of peptidoglycan was measured in DAPR CB1634 cells untreated and treated with DAP/OXA after separation by reverse phase HPLC. Analysis of the HPLC profiles revealed marked differences in CW cross-linking in CB1634 ± DAP/OXA (Fig. 5A), showing that exposure to DAP/OXA resulted in a significant decrease in the amount of highly cross-linked oligomer muropeptides (peaks # 17-22), which should reduce CW rigidity. These results are in accordance with our data showing that exposure of DAPR strains to DAP/OXA reduces the levels of PBP2a associated with the CM, which in turn could lead to the observed CW rearrangements and increased oxacillin susceptibility.

To investigate the role of *mprF* in CW composition, notably taking into account the observations described above, we compared muropeptide profiles of CB1634 with those of the CB1634 Δ*mprF* mutant. While no differences in profiles were observed between both strains in the absence of antibiotics (Fig. 5B, upper panels), the addition of OXA in the CB1634-Δ*mprF* strain, showed significantly enrichment for monomeric and dimeric components. These *mprF*-dependent effects were further enhanced by co-exposure to DAP/OXA (Fig. 5B, middle and lower panels, respectively), providing a plausible explanation for the ability of the *mprF* deletion in DAPR strains to reverse the increased susceptibility to OXA during the see-saw effect, as shown in Table 2.

Crosstalk between MprF and PrsA proteins. To understand further the molecular mechanism linking the *mprF*L826F mutation with decreased PBP2a levels in the CM and PG crosslinking during the see-saw effect, three basic observations were important to consider. First, we recently demonstrated that PrsA, a lipoprotein acting as a post-translocational chaperone, is involved in β-lactam resistance by affecting amounts of PBP2a in the CM (20); in addition, *prsA* expression is regulated by the two-component system VraSR (22). Second, we have shown that acquisition of DAPR involves upregulation of genes controlling CW synthesis and turnover, including *vraSR* (28).

325 Unpublished RNA-Seq results suggest that *vraSR* and *prsA* genes in the DAPR CB1634 strain are
326 up-regulated compared to the DAPS CB1631 strain, suggesting a link between the *mprF* (L826F)
327 mutation present in CB1634 and changes in the expression of both *vraSR* and *prsA* genes. Third,
328 MprF has been shown to be involved in the modification of the membrane phospholipid
329 phosphatidylglycerol, which in turn acts as a substrate for the Lgt enzyme that modifies lipoproteins
330 such as PrsA (46).
331 In light of these observations, we hypothesized that DAPR-associated *mprF* mutations could affect
332 the ability of PrsA to associate with the CM and consequently affect its functional activity. To test
333 whether PrsA and MprF are mutually interconnected during the DAPR-mediated see-saw effect, we
334 first evaluated cellular levels of PrsA and its localization in both CM and extracellular protein
335 extracts (Fig. 6). Consistent with the RNA-Seq analysis, we observed that steady state levels of PrsA
336 in the CM were higher in CB1634 vs. CB1631 (Fig. 6A). Interestingly, levels of PrsA, almost
337 undetectable in the absence of *mprF* (CB1634Δ*mpr*F), were restored by complementation with
338 *mprF*L826F (CB1634Δ*mprF*+ *mprF*L826F), but not by WT *mprF* (CB1634Δ*mprF*+*mprF*) (Fig.
339 6A). Concomitant analysis of OD_{600}-normalized extracellular extracts showed increased amounts of
340 extracellular PrsA in the corresponding CB1634Δ*mpr*F and CB1634Δ*mprF*+*mprF* (WT) strains,
341 while no extracellular PrsA was detected in extracts from the CB1634Δ*mprF*+*mprFL826F* strain
342 (Fig. 6A). These results strongly suggest that PrsA localization to the CM is altered by the *mprF*
343 mutation, and this in turn is associated with the DAPR phenotype.

344 **PrsA-mediated effects on CM-associated PBP2a are triggered by the *mprFL826F* mutation.**
345 Since DAP-mediated effects during the see-saw effect involve alterations in PBP2a levels in the
346 membrane (Fig. 4A) and taking into account the PrsA-mediated regulatory role in β-lactam
347 resistance via modulation of PBP2a (21), we hypothesized that during acquisition of DAPR, cell
348 membrane modifications triggered by mutations in *mprF* alter PrsA membrane localization and

consequently PBP2a membrane levels. To test this idea, we measured PBP2a and PrsA protein levels in CM extracts prepared from CB1634 (carrying *mprFL826F*) grown in the absence or presence of DAP, OXA and the DAP/OXA combination. As shown in the Western blot in Fig. 6B, PBP2a and PrsA membrane protein levels were induced upon OXA stress, but consistent with our hypothesis, the DAP/OXA combination resulted in decreased cell membrane levels of PBP2a that correlated with a concomitant reduction of PrsA. Taken together, our results strongly suggest that despite DAP/OXA-induced transcriptional up-regulation of *mecA*, *mprF*-dependent loss of CM-anchored PrsA results in depletion of PBP2a. Thus, the acquisition of DAPR via an *mprF*-dependent mechanism results in insufficient levels of PBP2a needed to sustain resistance to β-lactams, an effect mediated by altered cell membrane localization of PrsA.

Homogeneous DAPR MRSA strains do not display the see-saw effect without DAP induction. In previous studies, we reported that two DAPR strains, CB5036 and CB5014 with mutations at MprF located at the central domain, P314L and S377L respectively, did not display the DAP-mediated see-saw effect, i.e. their OXA MICs remained the same (512 µg/ml) in both DAPS/R paired strains (CB5035/CB5036 and CB5013/CB5014, respectively (29). However, as we described, the DAP/OXA combination was still effective against them (29). These strains are called homogeneous MRSA because they express a uniformly high level of β-lactam resistance, different from the heterogeneous MRSA strains (e.g., CB1634) whose cell populations are able to express differential levels of resistance and that are mostly associated with lower MICs (1-32 µg/ml).

We hypothesized that the absence of DAP selection prevented detection of the see-saw effect in these strains. We tested this idea by growing cultures of DAPR strain CB5014 in the presence of sub lethal (½ MIC) concentrations of DAP (2 µg/ml DAP, 50 mg/L Ca^{2+}), after which the adjusted inoculum was plated onto MH agar containing ½ MIC of DAP (2 µg/ml). OXA E-test strips were placed on the plates and incubated for 24 h, after which a pronounced decrease in the OXA MIC

from 512 µg/ml to 1 µg/ml was observed (Fig. 7A-B); this low-level DAP-induced strain will be referred as CB5014IndD. Similar results were obtained with DAPR strain CB5036 (data not shown). In support of these observations, PBP2a was detectable in membrane extracts from CB5014 grown O/N without DAP induction and then exposed to DAP/OXA, whereas in CB5014IndD under the same conditions, levels of the protein became almost undetectable (Fig. 7C). These results are consistent with the appearance of the DAP-mediated see-saw effect, as it was only displayed in the CB5014IndD strain. Furthermore, as previously shown for CB1634 (Fig.4A), the absence of PBP2a in cell membrane extracts collected from CB5014IndD was not related to a decrease in the transcription levels of *mecA* mRNA: in the presence of OXA, either alone or in combination with DAP, *mecA* expression was highly induced (~4-5.6 fold, respectively; Fig. 7D). CB5014 exposed to OXA or OXA/DAP also showed increased *mecA* expression, although to lower levels than those observed in CB5014IndD (Fig. 7D). Together, these data suggest that DAPR homogeneous MRSA relies upon DAP induction-mediated factors to express the see-saw phenotype.

Role of VraSR in the DAP-mediated see-saw effect. As mentioned, we previously demonstrated the critical role played by the VraSR two-component regulatory system in the acquisition of DAPR (36) Moreover, DAPR strains including the homogenous CB5014 and CB5035 expressed higher levels of *vraSR* than their corresponding DAPS counterparts (36). To further elucidate and understand the mechanistic role of DAP-induced *vraSR* expression and the see-saw effect, we overexpressed *vraSR* in the corresponding DAPS CB5013 (OXA MIC= 512 µg/ml) and CB1631 (OXA MIC= 32 µg/ml) strains. This resulted in *vraSR* expression levels similar to those observed in the corresponding DAPR counterparts CB5014 and CB1634, as determined by RT-PCR (data not shown). Phenotypic analyses performed by OXA E-test showed that CB5013+*vraSR* and CB1631+*vraSR* displayed both DAP-mediated see-saw effects, i.e. decreased DAP susceptibility (MICs to DAP: 4 µg/ml) and oxacillin resistance (MICs to OXA: 0.25/0.5 µg/ml, DS

397 CB5013+*vraSR* and CB1631+*vraSR*, respectively; Fig.8A). Moreover, analysis of *mprF* DNA
398 sequences in these strains revealed amino acid changes that were identical to those present in their
399 DAPR counterparts (S337L in CB5014 and L826F in CB1634), demonstrating that DAP-mediated
400 increased expression of *vraSR* leads to polymorphisms in *mprF*. To investigate further the potential
401 role of DAP-mediated increased *vraSR* expression in changes in antibiotic susceptibilities related to
402 the see-saw effect, we analyzed PBP2a levels in cell membrane lysates from CB5013+*vraSR* and
403 CB1631+*vraSR* overexpression strains. As depicted in Fig. 8B, increased PBP2a levels were
404 observed at baseline in CB5013+*vraSR* compared to those in the other strains. When exposed to
405 OXA alone, all strains showed increased amounts of cell membrane-associated PBP2a. Importantly
406 however, membrane-associated PBP2a was undetectable following exposure to DAP/OXA in both
407 strains expressing higher levels of *vraSR,* consistent with the see-saw effect described above.

408 To gain further insights on potential differences between the strains displaying see-saw effect, i.e.
409 CB1634 and CB5014IndD, we compared the overall gene expression profile by comparing RNA-
410 Seq data after exposure to OXA or DAP/OXA. Expression of approximately 322 genes was
411 significant altered ($p<0.05$ and over two-fold difference; Supplemental Table 1). Of these, relevant
412 observations comparing CB5014IndD (DAP/OXA) vs CB1634 (DAP/OXA) included upregulation
413 of *vraSR* mRNA levels (~6-folds), accompanied by increased expression of *vraSR* target genes
414 transcripts *pbp2* (~4 folds) and *sgtB* (~3.5folds). In addition, *mecA* mRNA was also highly
415 upregulated (~21 and 5 folds, DAP/OXA – OXA, respectively), as well as *mecI/mecRI (*~5 and 3
416 folds. Other genes included those coding for proteins involved in the synthesis of PG precursors
417 (*murA-G*, *femAB*, *mraW*, between 6 and 3.9 folds) while downregulated genes were associated to
418 other gene class families, i.e. biosynthesis and metabolic pathways as iron (*fer*, *fmhA*) and histidine
419 (*hisG, hisH*), gluconate (gntP/gntK). Together, these results provide strong evidence supporting the
420 key mechanistic role played by increased expression of *vraSR* following DAP exposure and its

implication in the process leading to acquisition of DAP resistance and the concomitant see-saw effect.

DISCUSSION

DAP targets the bacterial CM, causing rapid membrane depolarization and cell death (3). Decreased susceptibility to DAP in *S. aureus* has been reported leading to clinical failures in patients with MRSA deep side infections such as endocarditis and abscesses (14,23,25). Previously, we identified two major factors to mutually cooperate with acquisition of DAP resistance, one related to the cell membrane (*mrpF* mutations) and the second affecting cell wall factors (VraSR) (28). Moreover, we observed that the DAPR phenotype was accompanied with increased susceptibility to OXA, the so-called "see-saw" effect. Previously, a concomitant rise of vancomycin resistance with decreased β-lactams resistance has been reported in some clinical vancomycin intermediate *S. aureus* (VISA) and Vancomycin Resistant *S. aureus* (VRSA). In VISA strains the mechanism remains undefined with some strains showing excision of SCC *mec* carrying *mecA*, while in others *mecA* is retained (44,45). By contrast in VRSA strains loss of β-lactam resistance seems to be associated with the inability of PBP2a to utilize UDP-MurNAc-depsipetide (D-Ala-D-Lac) cell wall precursor produced in VRSA for transpeptidation, leaving PBP2 as essential for the synthesis of the abnormally structured cell wall (43). To date, the precise mechanism responsible for the see-saw effect mediated by DAP resistance in MRSA still remains to be elucidated.

Based on the present study, we postulate that DAP-induced *mprF* mutations at the CM level cause alterations that affect the localization and functions of important proteins involved in cell wall construction. In this context, it has been previously noted that sub-inhibitory concentrations of DAP induce aberrant and asymmetric division septa in *B. subtilis* (36), reinforcing the notion that DAP may target both the CM and CW. Working on the hypothesis that by targeting the CM, DAP perturbs

444 the lipid environment of membrane-bound enzymes involved in PG synthesis, moderately disrupting
445 CW assembly, we found that exposure of DAPR cells to a combination of DAP and β-lactams led to
446 delocalization of PG synthesis from the division septum, redistributing this activity around the cell
447 wall. We and others have observed that the "see-saw" effect is mainly achieved by β-lactams
448 targeting PBP1 and/or PBP2 that localize at the septum of *S. aureus,* and furthermore, that this effect
449 does not depend on other PG synthesis enzymes (39). Recently, it has been demonstrated that PG
450 synthesis in *S. aureus* can rely solely on PBP1 and PBP2 after removing seven of the nine PG
451 synthesis proteins (39). The observation that only β-lactams targeting PBP1 or PBP2 are capable of
452 killing cells during exposure to DAP/OXA supports the idea that perturbations to these proteins are
453 largely sufficient for the MRSA sensitization observed during the see-saw effect.
454 Importantly, we found that sensitization to β-lactams in DAPR strains containing mutant *mprF* alleles
455 was associated with decreased levels of cell membrane-associated PBP2a. MprF is involved in the
456 modification of phosphatidylglycerol, which acts as a substrate for Lgt to modify lipoproteins such as
457 PrsA with lipid moieties (46). The present evidence highlights potential mutual interactions between
458 MprF and PrsA during DAP-R. In fact, it is plausible to postulate that cell membrane modifications
459 triggered by DAPR-mediated mutated MprF may affect both PrsA location and chaperone functions
460 which are required for PBP2a folding. In support of the importance of post-transcriptional regulation,
461 we observed, despite increased transcription of *mecA* through *mec* regulatory elements, reduced
462 amounts of cell membrane-associated PBP2a in DAP/OXA treated cells. These findings are in
463 agreement with recent observations by Jousselin *et al.* suggesting that PBP2a is a related substrate of
464 PrsA (21), although we cannot rule out the possibility that PrsA may also influence the septal
465 localization of PBPs, specifically PBP1 and PBP2, which are associated with the "see-saw" effect
466 and are PrsA substrates in three Gram-positive pathogens (10).

We have previously established a role for the lipoprotein PrsA as an important mediator of both glycopeptide and oxacillin resistance, the latter through its effect on potential proper maturation of PBP2a (21,22). A consideration of MprF and the biosynthesis of lipoproteins such as PrsA suggests a plausible model to explain the see-saw effect linking DAP non-susceptibility and decreased resistance to certain antistaphylococcal β-lactams in MRSA strains (Fig. 9).

The integral membrane protein MprF uses cytosolic charged lysyl tRNA to lysinylate phosphatidylglycerol and subsequently flips lysyl phosphatidyl glycerol (L-PG) to the outer leaflet of the cytoplasmic membrane. Mutated MprF, showing enhanced enzymatic transferase and/or flippase activity, results in a significantly increased proportion of L-PG in the membrane compared to PG as well as the generation of membrane L-PG asymmetry by the selective accumulation of L-PG in the outer leaflet (5,24).

Prelipoproteins mature sequentially by secretion, lipidation of the lipobox cysteine embedded within the signal sequence by phosphatidylglycerol and Lgt acyl transferase, and finally signal sequence cleavage by Lsp (19,42). The study of LgtA in *E. coli* demonstrated that the *S. aureus* enzyme could fully compensate for the *E. coli* enzyme (37). Further high resolution X-ray structure and function analysis of the *E. coli* enzyme revealed mechanistic features consistent with an active site facing the periplasm and acquisition of phosphatidylglycerol substrate from the outer membrane leaflet (26). Phosphatidylglycerol is used as a substrate lipid by at least four enzymes: MprF, LtsA, Cls1/2, and Lgt to control the biosynthesis of L-PG, polymerization of lipoteichoic acid glycerol phosphate, cardiolipin, and lipidation of lipoproteins, respectively. Only LtsA is essential, indicating that the activites provided by the other enzymes using phosphatidylglycerol as a substrate are facultative. (24,46). Since LtsA governs an essential process mediating the production of lipoteichoic acid, it is reasonable to ask what permits lipobox lipidation to continue, if at all, in DAPR strains arising from

490 mutated MprF (or enhanced GraRS activity driving MprF production) as lysyl-PG accumulates and
491 phosphatidylglycerol diminishes in the outer membrane leaflet.
492 We hypothesize that disruption of lipoprotein anchorage by inhibition of Lgt-mediated acyl transfer
493 contributes to the see-saw mechanism. Our model predicts that proper function of PrsA in particular
494 is disrupted, and is in accordance with our experimental findings. Failure to produce sufficient
495 lipidated PrsA would impair PrsA-dependent post-translational maturation of PBP2a, allowing
496 transpeptidase activity to be susceptible to β-lactams. Of course we cannot exclude alternative
497 scenarios in which other lipoproteins such as DsbA could affect protein function (15), or the effects
498 of membrane electrostatic charge on membrane-associated sensory processes that regulate cell wall
499 biosynthesis (20). In support of the specific role of PrsA, we have produced a PrsA lipobox cysteine
500 mutant that we cannot detect in membrane extracts by western blot analysis, suggesting that it is
501 unstable and degraded, or fails to anchor and is lost (Jousselin, Renzoni, unpublished).
502 The intriguing observation that some DAPR strains do not display a see-saw effect unless they are
503 pre-induced with sub-lethal levels of DAP prompted us to investigate in more detail the role of
504 VraSR. Indeed, we found that overproduction of VraSR in DAPS strains decreased susceptibility
505 to DAP and increased susceptibility to β-lactams, similar to made with LiaFSR, a pivotal regulator
506 of DAPR in enterococci (11). In the absence of DAP, the three-component regulatory system
507 LiaFSR is turned 'OFF' by the negative interaction of LiaF with LiaS. LiaS responds to membrane
508 stress by phosphorylating LiaR, which leads to changes in the transcription of several downstream
509 operons that affect CM homeostasis (11). Interestingly, in enterococci it has been also
510 demonstrated the ability of several β-lactams, especially ampicillin (AMP); ceftaroline (CPT) and
511 ertapenem (ERT), in providing synergistic activity with DAP and preventing the emergence of
512 DAP non susceptibility (31,40).

In *S. aureus*, VraS belongs to a subfamily of kinases that sense cell envelope stress and do not contain extracellular sensor domains (27). Although the transmembrane helices of this subgroup have been proposed to be involved in stress sensing, the precise mechanism of VraS-like kinase activation remains unknown. We propose that exposure of DAP-R strains to DAP/OXA determines membrane structure reorganization by changes in phospholipid composition which may activate VraSR signaling by promoting VraS dimerization and downstream events including autophosphorylation of VraS, phosphorylation of VraR, and gene regulation. Based on our observations, we postulate that DAP induction as seen in the CB5014IndD strain may favor oligomerization of VraR, which in turn may form a constitutively activated tetramer with high affinity for DNA, even in the absence of phosphorylation, favoring the development of DAP resistance and the see-saw effect phenotype, as in heterogeneous DAPR CB1634. We are currently studying differences in VraR oligomerization among DAP-R clinical strains that may explain the differences between heterogeneous and homogeneous DAPR –MRSA.

In summary, the present study addresses the mechanistic bases and significance of sensitization to β-lactams linked to DAPR in clinical MRSA strains. The combination of DAP and β-lactams has gained increased acceptance for the treatment of MRSA infections produced by DAPR strains, resulting in clinical successes. We demonstrate that VraSR is a key determinant of DAP resistance, leading to mutations in *mprF* that may impair PrsA chaperone functions, which are required for post-transcriptional maturation of PBP2a; these effects may account for re-sensitization of DAPR strains to cell wall-specific β-lactams. Continued progress in understanding DAP's mode of action and its impact on CM/CW machinery will provide fundamental insights into MRSA biology and be potentially translated into the discovery of new therapeutic targets.

FUNDING INFORMATION

536 The authors on this study have no relevant financial interests to report. This study was funded in part
537 from Merck former Cubist Pharmaceuticals, Lexington, MA and from NIH grant (NIH-
538 R56AI102503- 01A1 AE. Rosato, PI) and the Swiss National Science Foundation grants (AR
539 310030-149762 and WLK 10030-146540).

540 **ACKNOWLEDGMENTS**

541 We acknowledged Mrs. Liliana Paz and Ms. Regina Fernandez for their contribution to this work.

542 # REFERENCES

543

544 1. **Arbeit, R. D., D. Maki, F. P. Tally, E. Campanaro, and B. I. Eisenstein**. 2004. The
545 safety and efficacy of daptomycin for the treatment of complicated skin and skin-
546 structure infections. Clin.Infect.Dis. **38**:1673-1681.

547 2. **Baltz, R. H.** 2009. Daptomycin: mechanisms of action and resistance, and biosynthetic
548 engineering. Curr.Opin.Chem.Biol. **13**:144-151.

549 3. **Baltz, R. H., V. Miao, and S. K. Wrigley**. 2005. Natural products to drugs: daptomycin
550 and related lipopeptide antibiotics. Nat.Prod.Rep. **22**:717-741.

551 4. **Bayer, A. S., N. N. Mishra, L. Chen, B. N. Kreiswirth, A. Rubio, and S. J. Yang**.
552 2015. Frequency and Distribution of Single Nucleotide Polymorphisms within mprF in
553 Methicillin-Resistant Staphylococcus aureus (MRSA) Clinical Isolates: Role in Cross-
554 Resistance between Daptomycin and Host Defense Antimicrobial Peptides.
555 Antimicrob.Agents Chemother. doi:AAC.00970-15 [pii];10.1128/AAC.00970-15 [doi].

556 5. **Bayer, A. S., T. Schneider, and H. G. Sahl**. 2013. Mechanisms of daptomycin
557 resistance in Staphylococcus aureus: role of the cell membrane and cell wall.
558 Ann.N.Y.Acad.Sci. **1277**:139-158. doi:10.1111/j.1749-6632.2012.06819.x [doi].

559 6. **Berti, A. D., G. Sakoulas, V. Nizet, R. Tewhey, and W. E. Rose**. 2013. beta-Lactam
560 antibiotics targeting PBP1 selectively enhance daptomycin activity against methicillin-
561 resistant Staphylococcus aureus. Antimicrob.Agents Chemother. **57**:5005-5012.
562 doi:AAC.00594-13 [pii];10.1128/AAC.00594-13 [doi].

563 7. **Berti, A. D., E. Theisen, J. D. Sauer, P. Nonejuie, J. Olson, J. Pogliano, G. Sakoulas,**
564 **V. Nizet, R. A. Proctor, and W. E. Rose**. 2015. Penicillin Binding Protein 1 Is
565 Important in the Compensatory Response of Staphylococcus aureus to Daptomycin-
566 Induced Membrane Damage and Is a Potential Target for beta-Lactam-Daptomycin
567 Synergy. Antimicrob.Agents Chemother. **60**:451-458. doi:AAC.02071-15
568 [pii];10.1128/AAC.02071-15 [doi].

569 8. **Bowker, K. E., H. A. Holt, R. J. Lewis, D. S. Reeves, and A. P. MacGowan**. 1998.
570 Comparative pharmacodynamics of meropenem using an in-vitro model to simulate once,
571 twice and three times daily dosing in humans. J.Antimicrob.Chemother. **42**:461-467.

572 9. **Boyle-Vavra, S., S. Yin, and R. S. Daum**. 2006. The VraS/VraR two-component
573 regulatory system required for oxacillin resistance in community-acquired methicillin-
574 resistant Staphylococcus aureus. FEMS Microbiol.Lett. **262**:163-171.

575 10. **Cahoon, L. A. and N. E. Freitag**. 2014. Listeria monocytogenes virulence factor
576 secretion: don't leave the cell without a chaperone. Front Cell Infect.Microbiol. **4**:13.
577 doi:10.3389/fcimb.2014.00013 [doi].

11. **Davlieva, M., Y. Shi, P. G. Leonard, T. A. Johnson, M. R. Zianni, C. A. Arias, J. E. Ladbury, and Y. Shamoo**. 2015. A variable DNA recognition site organization establishes the LiaR-mediated cell envelope stress response of enterococci to daptomycin. Nucleic Acids Res. **43**:4758-4773. doi:gkv321 [pii];10.1093/nar/gkv321 [doi].

12. **de Jonge, B. L., Y. S. Chang, D. Gage, and A. Tomasz**. 1992. Peptidoglycan composition of a highly methicillin-resistant Staphylococcus aureus strain. The role of penicillin binding protein 2A. J.Biol.Chem. **267**:11248-11254.

13. **Dhand, A., A. S. Bayer, J. Pogliano, S. J. Yang, M. Bolaris, V. Nizet, G. Wang, and G. Sakoulas**. 2011. Use of antistaphylococcal beta-lactams to increase daptomycin activity in eradicating persistent bacteremia due to methicillin-resistant Staphylococcus aureus: role of enhanced daptomycin binding. Clin.Infect.Dis. **53**:158-163. doi:cir340 [pii];10.1093/cid/cir340 [doi].

14. **Dubrac, S., I. G. Boneca, O. Poupel, and T. Msadek**. 2007. New insights into the WalK/WalR (YycG/YycF) essential signal transduction pathway reveal a major role in controlling cell wall metabolism and biofilm formation in Staphylococcus aureus. J.Bacteriol. **189**:8257-8269. doi:JB.00645-07 [pii];10.1128/JB.00645-07 [doi].

15. **Dumoulin, A., U. Grauschopf, M. Bischoff, L. Thony-Meyer, and B. Berger-Bachi**. 2005. Staphylococcus aureus DsbA is a membrane-bound lipoprotein with thiol-disulfide oxidoreductase activity. Arch.Microbiol. **184**:117-128. doi:10.1007/s00203-005-0024-1 [doi].

16. **Friedman, L., J. D. Alder, and J. A. Silverman**. 2006. Genetic changes that correlate with reduced susceptibility to daptomycin in Staphylococcus aureus. Antimicrob.Agents Chemother. **50**:2137-2145.

17. **Hachmann, A. B., E. R. Angert, and J. D. Helmann**. 2009. Genetic analysis of factors affecting susceptibility of Bacillus subtilis to daptomycin. Antimicrob.Agents Chemother. **53**:1598-1609.

18. **Hebert, L., P. Courtin, R. Torelli, M. Sanguinetti, M. P. Chapot-Chartier, Y. Auffray, and A. Benachour**. 2007. Enterococcus faecalis constitutes an unusual bacterial model in lysozyme resistance. Infect.Immun. **75**:5390-5398. doi:IAI.00571-07 [pii];10.1128/IAI.00571-07 [doi].

19. **Hutchings, M. I., T. Palmer, D. J. Harrington, and I. C. Sutcliffe**. 2009. Lipoprotein biogenesis in Gram-positive bacteria: knowing when to hold 'em, knowing when to fold 'em. Trends Microbiol. **17**:13-21. doi:S0966-842X(08)00266-7 [pii];10.1016/j.tim.2008.10.001 [doi].

20. **Hyyrylainen, H. L., M. Pietiainen, T. Lunden, A. Ekman, M. Gardemeister, S. Murtomaki-Repo, H. Antelmann, M. Hecker, L. Valmu, M. Sarvas, and V. P. Kontinen**. 2007. The density of negative charge in the cell wall influences two-component signal transduction in Bacillus subtilis. Microbiology **153**:2126-2136. doi:153/7/2126 [pii];10.1099/mic.0.2007/008680-0 [doi].

21. **Jousselin, A., C. Manzano, A. Biette, P. Reed, M. Pinho, A. Rosato, W. L. Kelley, and A. Renzoni**. 2015. The Staphylococcus aureus chaperone PrsA is a new auxiliary factor of oxacillin resistance affecting Penicillin-binding protein 2A. Antimicrob.Agents Chemother. doi:AAC.02333-15 [pii];10.1128/AAC.02333-15 [doi].

22. **Jousselin, A., A. Renzoni, D. O. Andrey, A. Monod, D. P. Lew, and W. L. Kelley**. 2012. The posttranslocational chaperone lipoprotein PrsA is involved in both glycopeptide and oxacillin resistance in Staphylococcus aureus. Antimicrob.Agents Chemother. **56**:3629-3640. doi:AAC.06264-11 [pii];10.1128/AAC.06264-11 [doi].

23. **Julian, K., K. Kosowska-Shick, C. Whitener, M. Roos, H. Labischinski, A. Rubio, L. Parent, L. Ednie, L. Koeth, T. Bogdanovich, and P. C. Appelbaum**. 2007. Characterization of a daptomycin-nonsusceptible vancomycin-intermediate Staphylococcus aureus strain in a patient with endocarditis. Antimicrob.Agents Chemother. **51**:3445-3448.

24. **Kuhn, S., C. J. Slavetinsky, and A. Peschel**. 2015. Synthesis and function of phospholipids in Staphylococcus aureus. Int.J.Med.Microbiol. **305**:196-202. doi:S1438-4221(14)00175-1 [pii];10.1016/j.ijmm.2014.12.016 [doi].

25. **Mangili, A., I. Bica, D. R. Snydman, and D. H. Hamer**. 2005. Daptomycin-resistant, methicillin-resistant Staphylococcus aureus bacteremia. Clin.Infect.Dis. **40**:1058-1060. doi:CID34447 [pii];10.1086/428616 [doi].

26. **Mao, G., Y. Zhao, X. Kang, Z. Li, Y. Zhang, X. Wang, F. Sun, K. Sankaran, and X. C. Zhang**. 2016. Crystal structure of E. coli lipoprotein diacylglyceryl transferase. Nat.Commun. **7**:10198. doi:ncomms10198 [pii];10.1038/ncomms10198 [doi].

27. **Mascher, T., J. D. Helmann, and G. Unden**. 2006. Stimulus perception in bacterial signal-transducing histidine kinases. Microbiol.Mol.Biol.Rev. **70**:910-938. doi:70/4/910 [pii];10.1128/MMBR.00020-06 [doi].

28. **Mehta, S., A. X. Cuirolo, K. B. Plata, S. Riosa, J. A. Silverman, A. Rubio, R. R. Rosato, and A. E. Rosato**. 2011. VraSR two-component regulatory system contributes to mprF-mediated decreased susceptibility to daptomycin in-vivo-selected MRSA clinical strains. Antimicrob.Agents Chemother. doi:AAC.00432-10 [pii];10.1128/AAC.00432-10 [doi].

29. **Mehta, S., C. Singh, K. B. Plata, P. K. Chanda, A. Paul, S. Riosa, R. R. Rosato, and A. E. Rosato**. 2012. beta-lactams increase the antibacterial activity of daptomycin against clinical MRSA strains and prevent selection of DAP-resistant derivatives. Antimicrob.Agents Chemother. doi:AAC.01525-12 [pii];10.1128/AAC.01525-12 [doi].

30. **Moise, P. A., M. Amodio-Groton, M. Rashid, K. C. Lamp, H. L. Hoffman-Roberts, G. Sakoulas, M. J. Yoon, S. Schweitzer, and A. Rastogi**. 2013. Multicenter evaluation of the clinical outcomes of daptomycin with and without concomitant beta-lactams in patients with Staphylococcus aureus bacteremia and mild to moderate renal impairment. Antimicrob.Agents Chemother. **57**:1192-1200. doi:AAC.02192-12 [pii];10.1128/AAC.02192-12 [doi].

31. **Munita, J. M., D. Panesso, L. Diaz, T. T. Tran, J. Reyes, A. Wanger, B. E. Murray, and C. A. Arias**. 2012. Correlation between mutations in liaFSR of Enterococcus faecium and MIC of daptomycin: revisiting daptomycin breakpoints. Antimicrob.Agents Chemother. **56**:4354-4359. doi:AAC.00509-12 [pii];10.1128/AAC.00509-12 [doi].

32. National Commitee for Clinical Laboratory Standards. Performance standards for antimicrobial disk susceptibility tests. Approved standard M2-A8. 8th. 2007. Wayne, PA. Ref Type: Generic

33. **NNIS System, A. r. f. t.** 2004. National Nosocomial Infections Surveillance (NNIS) System Report, data summary from January 1992 through June 2004, issued October 2004. American Journal of Infection Control **32**:470-485. doi:doi: 10.1016/j.ajic.2004.10.001.

34. **Pillai, D. R., R. Melano, P. Rawte, S. Lo, N. Tijet, M. Fuksa, N. Roda, D. J. Farrell, and S. Krajden**. 2009. Klebsiella pneumoniae Carbapenemase, Canada. Emerg.Infect.Dis. **15**:827-829. doi:10.3201/eid1505.081536 [doi].

35. **Pinho, M. G. and J. Errington**. 2005. Recruitment of penicillin-binding protein PBP2 to the division site of Staphylococcus aureus is dependent on its transpeptidation substrates. Mol.Microbiol. **55**:799-807. doi:MMI4420 [pii];10.1111/j.1365-2958.2004.04420.x [doi].

36. **Pogliano, J., N. Pogliano, and J. A. Silverman**. 2012. Daptomycin-mediated reorganization of membrane architecture causes mislocalization of essential cell division proteins. J.Bacteriol. **194**:4494-4504. doi:JB.00011-12 [pii];10.1128/JB.00011-12 [doi].

37. **Qi, H. Y., K. Sankaran, K. Gan, and H. C. Wu**. 1995. Structure-function relationship of bacterial prolipoprotein diacylglyceryl transferase: functionally significant conserved regions. J.Bacteriol. **177**:6820-6824.

38. **Rand, K. H. and H. J. Houck**. 2004. Synergy of daptomycin with oxacillin and other beta-lactams against methicillin-resistant Staphylococcus aureus. Antimicrob.Agents Chemother. **48**:2871-2875. doi:10.1128/AAC.48.8.2871-2875.2004 [doi];48/8/2871 [pii].

39. **Reed, P., M. L. Atilano, R. Alves, E. Hoiczyk, X. Sher, N. T. Reichmann, P. M. Pereira, T. Roemer, S. R. Filipe, J. B. Pereira-Leal, P. Ligoxygakis, and M. G. Pinho**. 2015. Staphylococcus aureus Survives with a Minimal Peptidoglycan Synthesis Machine but Sacrifices Virulence and Antibiotic Resistance. PLoS.Pathog. **11**:e1004891. doi:10.1371/journal.ppat.1004891 [doi];PPATHOGENS-D-14-02400 [pii].

40. **Sakoulas, G., P. Nonejuie, V. Nizet, J. Pogliano, N. Crum-Cianflone, and F. Haddad**. 2013. Treatment of high-level gentamicin-resistant Enterococcus faecalis endocarditis with daptomycin plus ceftaroline. Antimicrob.Agents Chemother. **57**:4042-4045. doi:AAC.02481-12 [pii];10.1128/AAC.02481-12 [doi].

41. **Samra, Z., O. Ofir, Y. Lishtzinsky, L. Madar-Shapiro, and J. Bishara**. 2007. Outbreak of carbapenem-resistant Klebsiella pneumoniae producing KPC-3 in a tertiary

medical centre in Israel. Int.J.Antimicrob.Agents **30**:525-529. doi:S0924-8579(07)00374-3 [pii];10.1016/j.ijantimicag.2007.07.024 [doi].

42. **Sankaran, K. and H. C. Wu**. 1994. Lipid modification of bacterial prolipoprotein. Transfer of diacylglyceryl moiety from phosphatidylglycerol. J.Biol.Chem. **269**:19701-19706.

43. **Severin, A., S. W. Wu, K. Tabei, and A. Tomasz**. 2004. Penicillin-binding protein 2 is essential for expression of high-level vancomycin resistance and cell wall synthesis in vancomycin-resistant Staphylococcus aureus carrying the enterococcal vanA gene complex. Antimicrob.Agents Chemother. **48**:4566-4573. doi:48/12/4566 [pii];10.1128/AAC.48.12.4566-4573.2004 [doi].

44. **Sieradzki, K., T. Leski, J. Dick, L. Borio, and A. Tomasz**. 2003. Evolution of a vancomycin-intermediate Staphylococcus aureus strain in vivo: multiple changes in the antibiotic resistance phenotypes of a single lineage of methicillin-resistant S. aureus under the impact of antibiotics administered for chemotherapy. J.Clin.Microbiol. **41**:1687-1693.

45. **Sieradzki, K. and A. Tomasz**. 1999. Gradual alterations in cell wall structure and metabolism in vancomycin-resistant mutants of Staphylococcus aureus. J.Bacteriol. **181**:7566-7570.

46. **Stoll, H., J. Dengjel, C. Nerz, and F. Gotz**. 2005. Staphylococcus aureus deficient in lipidation of prelipoproteins is attenuated in growth and immune activation. Infect.Immun. **73**:2411-2423. doi:73/4/2411 [pii];10.1128/IAI.73.4.2411-2423.2005 [doi].

47. **Turner, R. D., A. F. Hurd, A. Cadby, J. K. Hobbs, and S. J. Foster**. 2013. Cell wall elongation mode in Gram-negative bacteria is determined by peptidoglycan architecture. Nat.Commun. **4**:1496. doi:ncomms2503 [pii];10.1038/ncomms2503 [doi].

48. **Turner, R. D., E. C. Ratcliffe, R. Wheeler, R. Golestanian, J. K. Hobbs, and S. J. Foster**. 2010. Peptidoglycan architecture can specify division planes in Staphylococcus aureus. Nat.Commun. **1**:26. doi:ncomms1025 [pii];10.1038/ncomms1025 [doi].

49. **Yang, S. J., Y. Q. Xiong, S. Boyle-Vavra, R. Daum, T. Jones, and A. S. Bayer**. 2010. Daptomycin-oxacillin combinations in treatment of experimental endocarditis caused by daptomycin-nonsusceptible strains of methicillin-resistant Staphylococcus aureus with evolving oxacillin susceptibility (the "seesaw effect"). Antimicrob.Agents Chemother. **54**:3161-3169. doi:AAC.00487-10 [pii];10.1128/AAC.00487-10 [doi].

731 **LEGENDS TO FIGURES**

732 **Fig 1. Effects of DAP on cytoplasmic membrane and cell wall** of **A)** DAPS CB1631 or **B)** DAPR
733 CB1634 bacterial strains. Bacteria were grown in TSB (±DAP) at 37 ˚C to late exponential phase
734 (2.5 hours) and labelled for 5 minutes with FM1-43FX (membrane; upper panels), bocillin-
735 vancomycin (D-alanyl-D-alanine, cell division; middle panels) and HADA (peptidoglycan insertion;
736 lower panels). A Nikon inverted epifluorescence microscope was used. Exposure and contrast
737 settings were optimised per image, i.e. brightness is not comparable between fields).

738 **Fig. 2. Localization of PBP2-GFP fusions in DAPR cells treated with OXA, DAP, or**
739 **DAP/OXA.** **A**) The DAPR-CB1634 strain producing PBP2-GFP was grown ± sublethal
740 concentrations of DAP/OXA (1/2 MIC), followed by labelling with BodipyFL-VAN, fixation, and
741 imaging by fluorescence microscopy. **B)** DAPR-CB1634 cells producing PBP2a-GFP were induced
742 with IPTG in the presence or absence of DAP, OXA or the DAP/OXA combination, fixed, and
743 imaged by fluorescence microscopy.

744 **Fig. 3. Analysis of PBPs from CB1634 cells treated with OXA, DAP or DAP/OXA.** Detection
745 of penicillin binding proteins PBP1, PBP2, PBP3 and PBP4 in membrane preparations obtained from
746 CB1634 cells untreated and treated with OXA (0.5µg/ml), DAP (1µg /ml) and DAP /OXA (0.5
747 µg/ml /1 µg/ml). Equal amounts (20 µg) of Bocillin-FL labelled membrane proteins were separated
748 by 10% SDS-PAGE. Fluorescently labelled PBPs are indicated by arrows.

749 **Fig 4. Sensitization to β-lactams during DAP resistance is associated with decreased**
750 **production of PBP2a.** **A)** Western blot analysis of PBP2a protein in membrane and extracellular
751 protein extracts from DAPR-CB1634 grown without (C = control) or with DAP, OXA or DAP/OXA
752 combination. Carbonic anhydrase was used a loading control. **B)** RT-PCR analysis showing *mecA*

753 gene expression in DAPR-CB1634 grown without or with DAP, OXA or DAP/OXA combination; *:
754 significantly higher than CB1634 control (no antibiotic), p< 0.05; # significantly higher than cells
755 exposed to DAP or OXA alone, p< 0.05. **C)** Western blot analysis of PBP2a protein in membrane
756 protein extracts from CB1643*ΔmprF* (MAR17*)*, CB1634*ΔmprF+mprF*(WT)(MAR18) and
757 CB1634*ΔmprF+mprFL826F* (MAR19) grown without (C) or with DAP, OXA or DAP/OXA
758 combination.

759 **FIG 5** (A) Effect of DAP/OXA combination on peptidoglycan crosslinking. Peptidoglycan
760 muropeptide composition was analyzed by reverse phase HPLC from DAPR-CB1634 strains grown
761 without or with DAP/OXA combination. Peaks numbered 17-22 denote highly cross-linked oligomer
762 muropeptides. (B) Effect of *mprF* deletion on peptidoglycan crosslinking in presence of OXA or
763 DAP/OXA combination. Peptidoglycan muropeptide composition was analyzed by reverse phase
764 HPLC from DAPR-CB1634 (left panels) and DAPS-CB1634Δ*mprF* (right panels) strains grown
765 without or with OXA or DAP/OXA combination.

766 **FIG 6** Effect of *mprF* mutations on PrsA membrane localization. (A) Western blot analysis of PrsA
767 protein in membrane protein extracts (upper panel) and extracellular protein extracts (lower panel)
768 from DAPS-CB1631, DAPR-CB1634, CB1643*ΔmprF*, *CB1634ΔmprF+mprF*(WT) and
769 CB1634*ΔmprF+mprFL826F* grown without antibiotics. Carbonic anhydrase was used a loading
770 control. (B) Western Blot analysis of PBP2a and PrsA in membrane extracts and from DAPR-
771 CB1634 grown without (C = control) or with OXA, DAP or DAP/OXA combination.

772 **FIG 7** Homogeneous DAPR MRSA strains do not display the see-saw effect without DAP
773 induction. DAPR strain CB5014 grown overnight (O/N) in the absence (A) and in the presence (B),
774 CB5014indD) of sublethal concentrations of DAP (½ MIC; 2µg/ml 50 mg/L Ca^2), after which the
775 adjusted inoculum was plated onto MH agar containing ½ MICs DAP (2 µg/ml). OXA E-test strips

776 were placed on the plates, and incubated for 24 h. (C) Western blot analysis of PBP2a present in cell
777 membrane extracts collected from cells as described in (A). (D) Quantitation of *mecA* mRNA by
778 real-time RT-PCR using RNA prepared from CB5014 and CB5014IndD; relative fold changes are
779 shown; 16S rRNA: internal control. #/*: significantly higher than Control, P<0.05/0.01, respectively.

780 **FIG 8** VraSR and DAP-mediated see-saw effect. (A) CB5013+*vraSR* and CB1631+*vraSR* strains
781 were grown O/N after which the adjusted inoculum was plated onto MH agar and OXA Etest strips
782 were placed on the plates, and incubated at 37°C for 24 h. (B) western blot analysis of PBP2a present
783 in cell membrane extracts collected under the indicated conditions in DAPS CB5013 and CB1631,
784 and their corresponding +*vraSR* counterparts (CB5013+*vraSR* and CB1631+*vraSR,* respectively).

785 **FIG 9.** Proposed model of MprF (A) or mutated MprF* (B) affecting lipoprotein PrsA anchorage. 1.
786 MprF uses cytosolic lysyl tRNA to convert phosphatidyl glycerol (PG) to lysyl phosphatidyl
787 glycerol (L-PG). 1b. Enhanced transferase and/or flippase activity of mutated MprF increases the
788 proportion of L-PG compared to PG in the outer membraned leaflet. 2. Prelipoprotein PrsA is
789 secreted probably through Sec pathway. 3. PG is used by Lgt enzyme to lipid-modify the PrsA
790 lipobox cysteine. 3b. Inhibition of Lgt-mediated acyl transfer to PrsA due to increased L-PG/reduced
791 phosphatidylglycerol amounts in the outer membrane leaflet. 4. Lipidated membrane-anchored PrsA
792 will help post-translational maturation of PBP2A. 4b. Failure to produce lipidated membrane-
793 anchored PrsA.

794

795

796

797

798

799 **Table 1**. Strains and plasmids used in this study

Strain or plasmid	Description	Reference
CB5011	Daptomycin susceptible	(28)
CB5012	Daptomycin resistant isogenic to CB5011; *mprF* L826F	(28)
CB5013	Daptomycin susceptible	(28)
CB5014	Daptomycin resistant isogenic to CB5013; *mprF* S377L	(28)
CB1631	Daptomycin susceptible	(28)
CB1634	Daptomycin resistant isogenic to CB1631; *mprf* L826F	(28)
MAR-17	CB1634 Δ*mprF::cat*	(28)
MAR-18	MAR-17 + pMPRF-1 (wild type)	(28)
MAR-19	MAR-17 + pMPRF-2 (L826F mutant)	(28)
5013 +VraSR	Entire *vraS/vraR* cloned into pAW8	This study
1631 +VraSR	*vraS/vraR* cloned into pAW8	and (9)
	Primers and probes	
PrsA-F	AGTTAATGATAAGAAGATTGACGA	
PrsA-R	GAAGGGCCTTTTCAAATTTATCTTT	
VraSR-F	GGTGCAACGTTCCCATATTGTATTGT	
VraSR-R	GGCTTCAACTCATGGGCTTTGGCAA	

mprF-F	GGTGGCTTTATTGGTGCAGGCG
mprF-R	GATGCATCGAAAACATGGAA
mecA-F	TGCCTAATCTCATTGTGTTCCTGTAT
mecA-R	CGGTGCTGAAACTTTCACAATATAAT
pbp2-GFPF (DPH407)	GATAGCGGCCGCATGACGGAAAACAAAGGATCTTCTC
pbp2-GFPR (DPH408)	GAAGGGATCCTTAGTTGAATATACCTGTTAATCCACCG
16S-F	TCCGGAATTATTGGGCGTAA
16S-R	CCACTTTCCTCTTCTGCACTCA

800

801 **Table 2.** Minimal inhibitory concentrations (MICs) of DAPR CB1634 and *mprF*-derivatives for
802 daptomycin (DAP) and oxacillin (OXA) as determined by Etest.

803

Strains	MIC (µg/ml)	
	DAP	OXA
CB1634	4	0.5
CB1634Δ*mprF*	0.25	32
CB1634Δ*mprF*+*mprF(WT)*	0.75	32
CB1634Δ*mprF*+*mprF*(L826F)	3	1

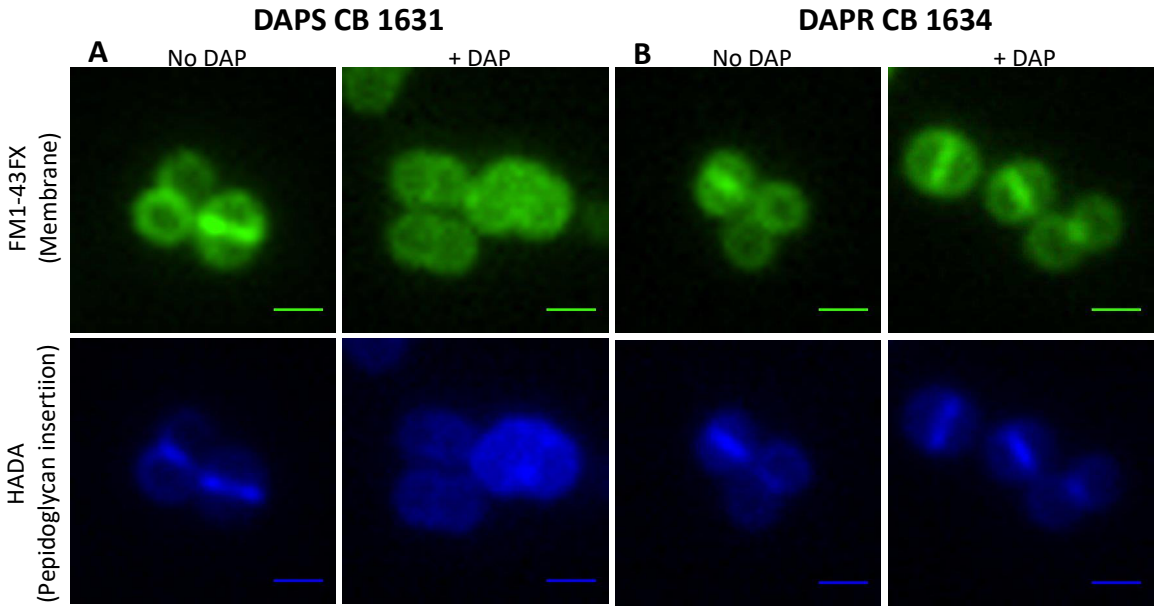

Fig 1. Daptomycin effects on cytoplamic membrane and cell wall. DAPS CB1631 and DAPR CB1634 strains were grown in TSB (±DAP) at 37 ˚C to late exponential phase (2.5 hours) and labelled for 5 minutes with FM1-43FX (membrane; **A**) or HADA (peptidoglycan insertion; **B**). A Nikon inverted epifluorescence microscope was used. Exposure and contrast settings were optimized per image, i.e. brightness is not comparable between fields. Scale bars are 1 µm.

Fig 2

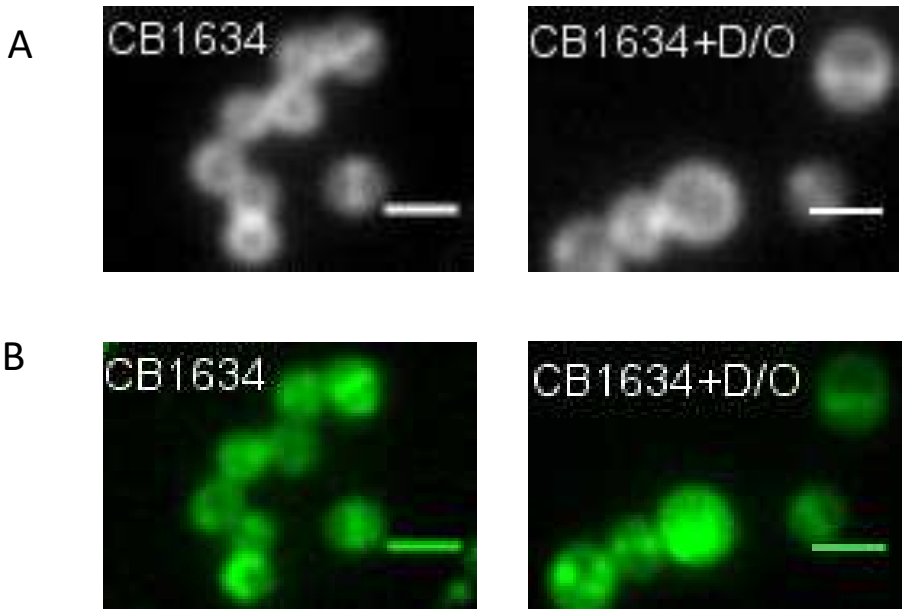

Fig. 2. **Fluorescence microscopy analysis** of: **A**) DAPR-CB1634 strain grown ± sublethal concentrations of DAP/OXA (1/2 MIC), followed by labelling with BodipyFL-VAN, fixation, and after mounting on slides, imaged using Deltavision microscope. **B)** DAPR-CB1634-*pbp2/gfp* induced with IPTG in the presence or absence of DAP, OXA or DAP/OXA combination.

Fig 3

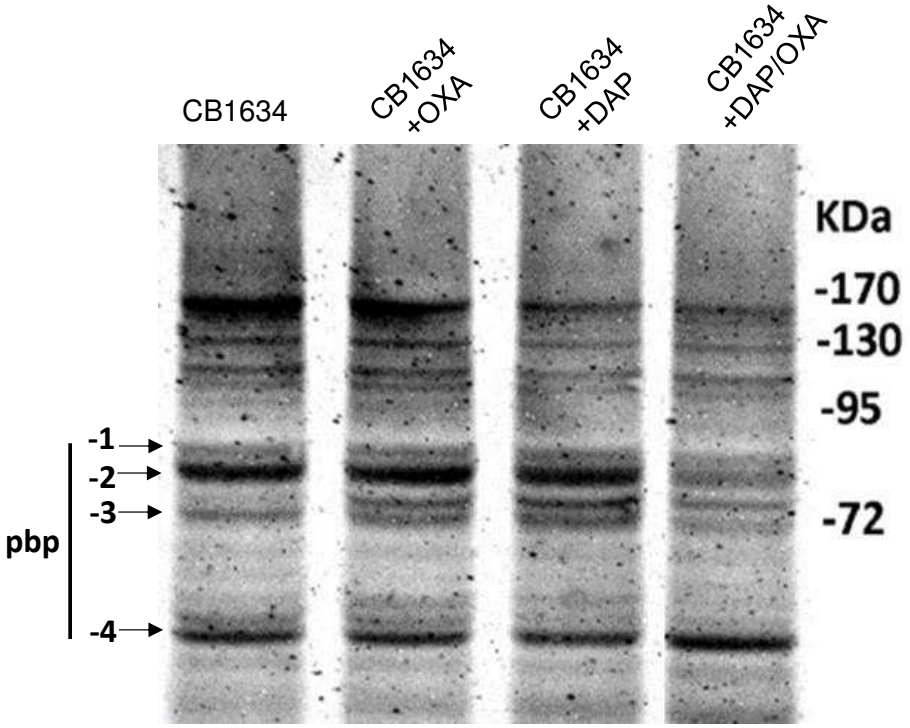

Fig. 3. **PBPs analysis in CB1634 cells undergoing treatment with OXA, DAP and DAP/OXA.** Detection of penicillin binding proteins PBP1, PBP2, PBP3 and PBP4 in membrane preparations obtained from CB1634 cells untreated and treated with OXA (0.5 µg/ml), DAP (1µg /ml) and DAP /OXA (0.5 µg/ml /1 µg/ml). Equal amounts (20 µg) of Bocillin-FL labelled membrane proteins were separated on 10% SDS-Page gel. Fluorescently labelled PBPs are indicated by arrows.

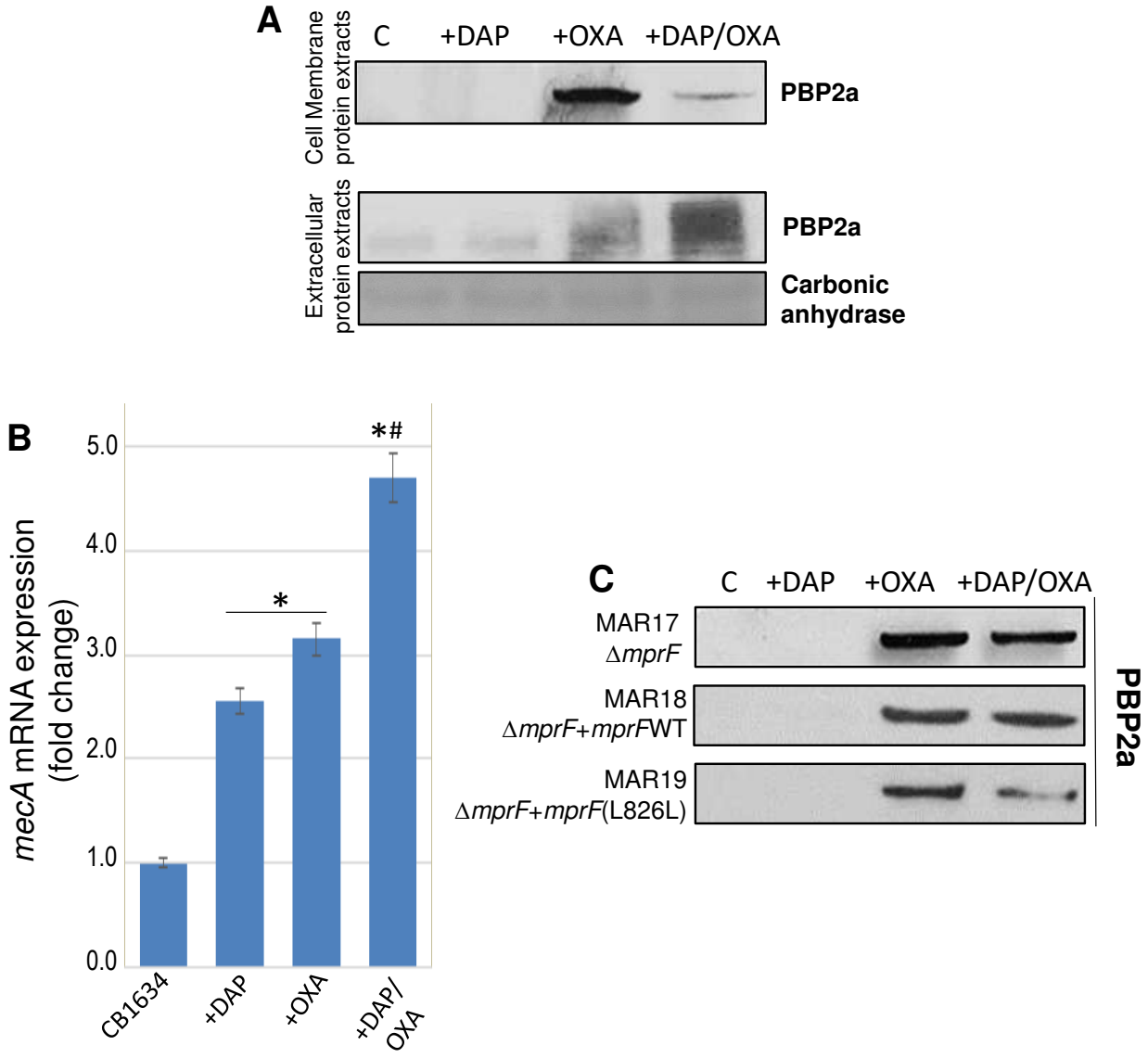

Fig. 4. A) Western blot analysis of PBP2A protein in membrane and extracellular protein extracts from DAPR-CB1634 grown without (C = control) or with DAP, OXA or DAP/OXA combination. **B)** RT-PCR analysis showing *mecA* gene expression in DAPR-CB1634 grown without or with DAP, OXA or DAP/OXA combination; *: significantly higher than CB1634 control (no antibiotic), $p< 0.05$; # significantly higher than cells exposed to DAP or OXA alone, $p< 0.005$. **C)** Western blot analysis of PBP2A protein in membrane protein extracts from CB1643*ΔmprF* (MAR17*)*, CB1634*ΔmprF+mprF*(WT)(MAR18) and CB1634*ΔmprF+mprF*(L826F)(MAR19) grown without (C) or with DAP, OXA or DAP/OXA combination.

A

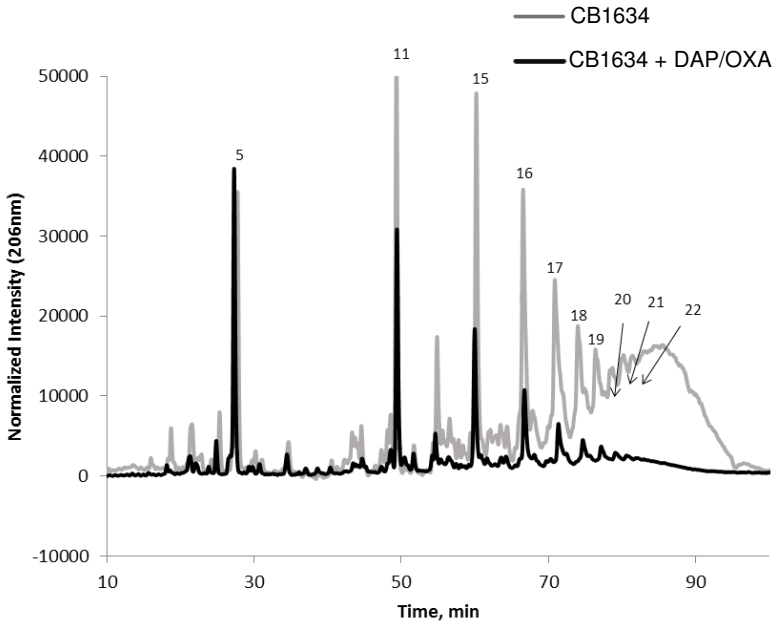

Fig. 5. A) Effect of DAP/OXA combination on peptidoglycan crosslinking. Peptidoglycan muropeptide composition was analyzed by reverse phase HPLC from DAPR-CB1634 strains grown without or with DAP/OXA combination. Numbers 17-22 denoted highly cross-linked oligomer muropeptides.

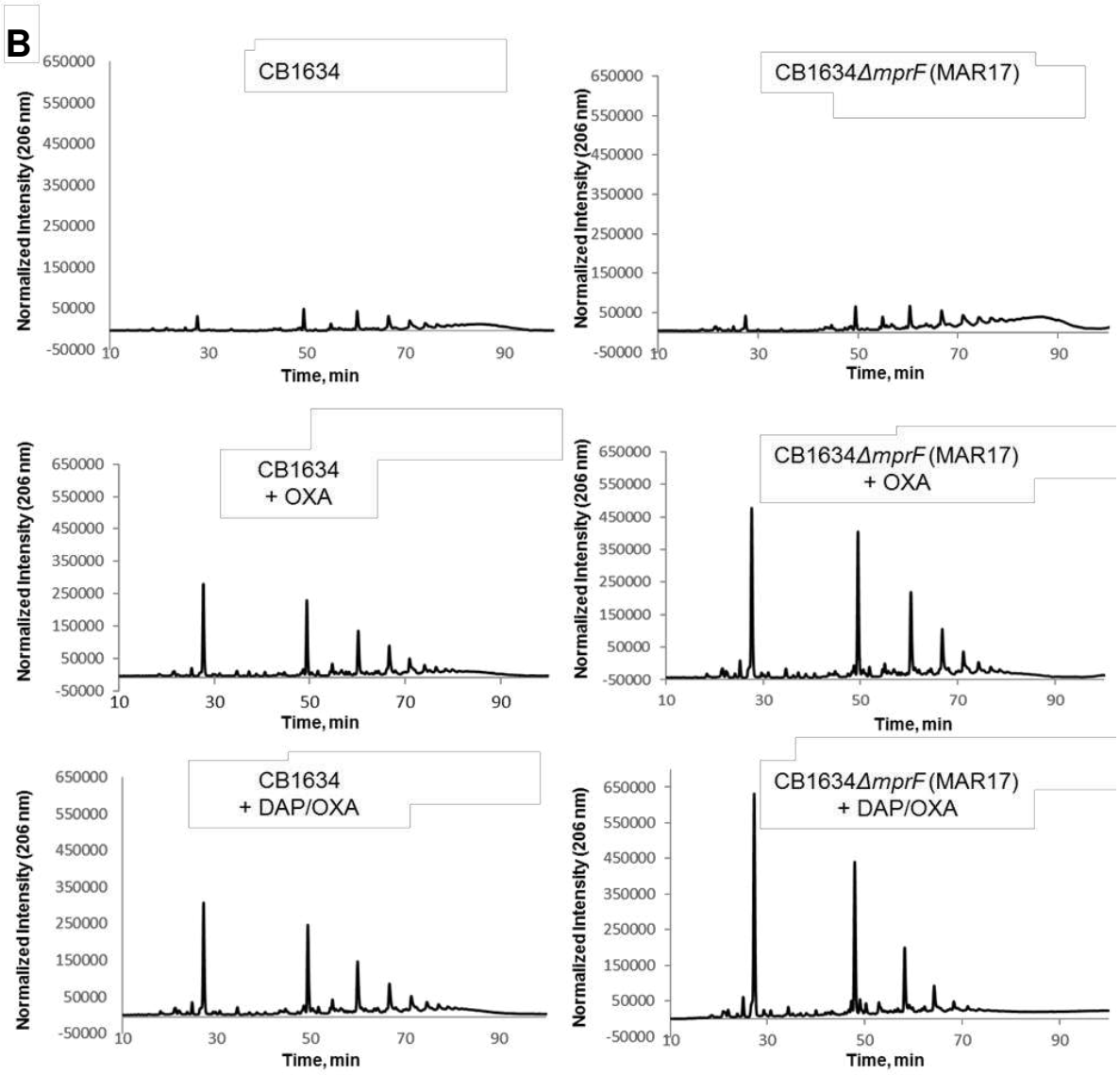

Fig. 5.. B) Effect of *mprF* deletion on peptidoglycan crosslinking in the presence of OXA or DAP/OXA combination. Peptidoglycan muropeptide composition was analyzed by reverse phase HPLC from DAPR-CB1634 and DAPS-CB1634Δ*mprF* strains grown without or with OXA or DAP/OXA combination.

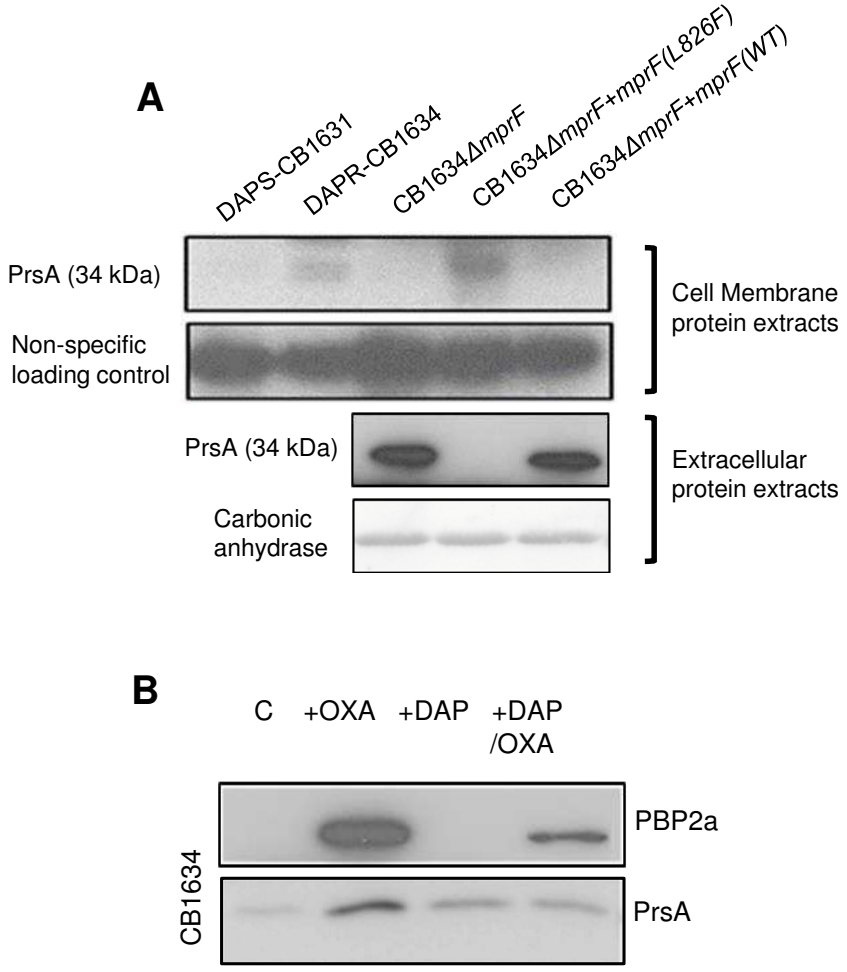

Fig 6. Effect of *mprF* mutations on PrsA membrane localization. **(A)** Western blot analysis of PrsA protein in membrane protein extracts (upper panel) and extracellular protein extracts (lower panel) from DAPS-CB1631, DAPR-CB1634, CB1643*ΔmprF*, CB1634*ΔmprF+mprF*(WT) and CB1634*ΔmprF+mprF*(L826F) grown without antibiotics. Carbonic anhydrase was used a loading control. (**B)** Western blot analysis of PBP2a and PrsA in membrane extracts prepared from DAPR-CB1634 grown without (C = control) or with OXA, DAP or DAP/OXA combination.

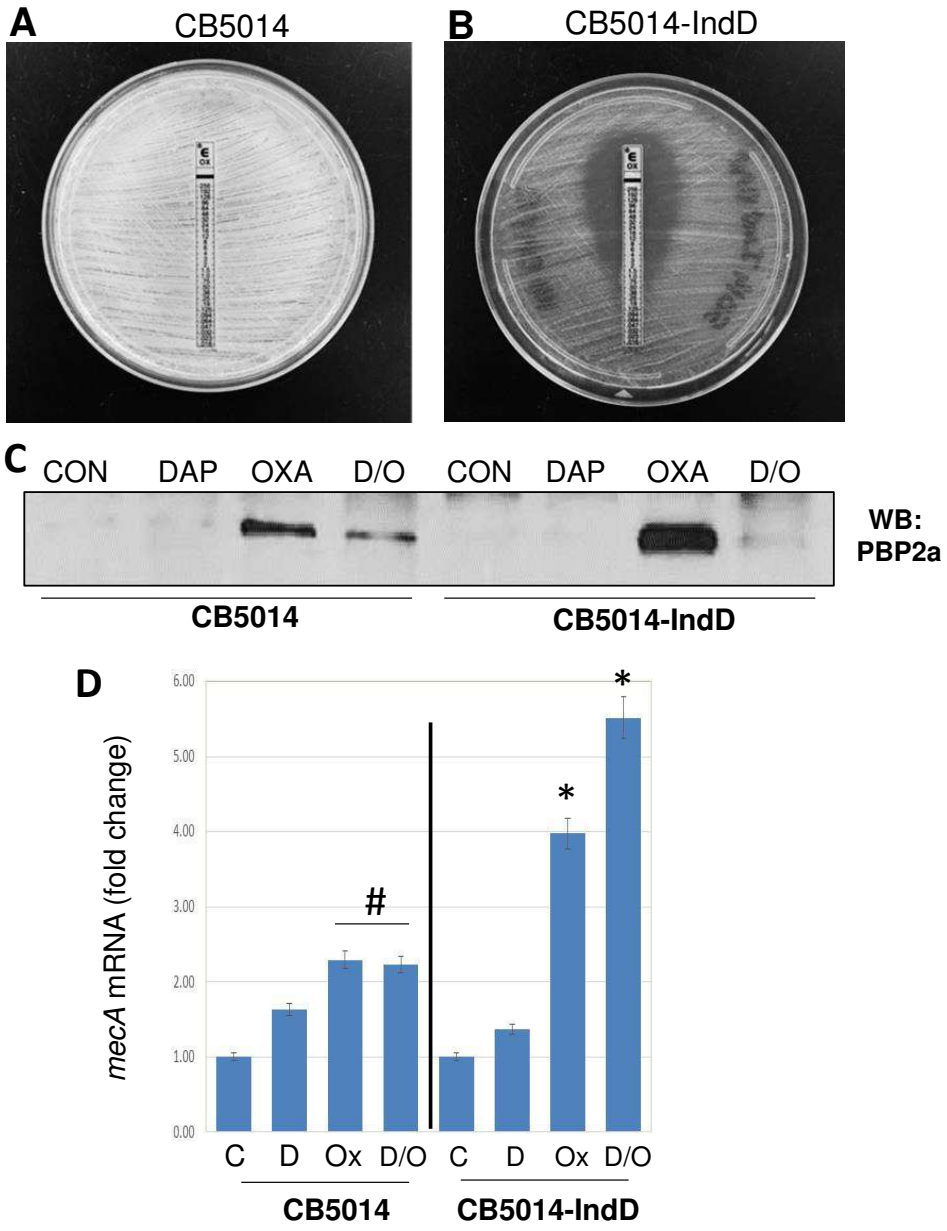

Fig 7. **Homogeneous DAPR MRSA strains do not display the see-saw effect without DAP induction.** DAPR strain CB5014 grown overnight (O/N) in the absence (A) and in the presence (B, CB5014indD) of sublethal concentrations of DAP (½ MIC; 2µg/ml 50 mg/L Ca^2), after which the adjusted inoculum was plated onto MH agar containing ½ MICs DAP (2 µg/ml). OXA E-test strips were placed on the plates, and incubated for 24 h. (C) western blot analysis of PBP2a present in cell membrane extracts collected from cells as described in (A). (D) Quantitation of *mecA* mRNA by real-time RT-PCR using RNA prepared from CB5014 and CB5014IndD; relative fold changes are shown; 16S rRNA: internal control. #/*: significantly higher than Control, P<0.05/0.01, respectively.

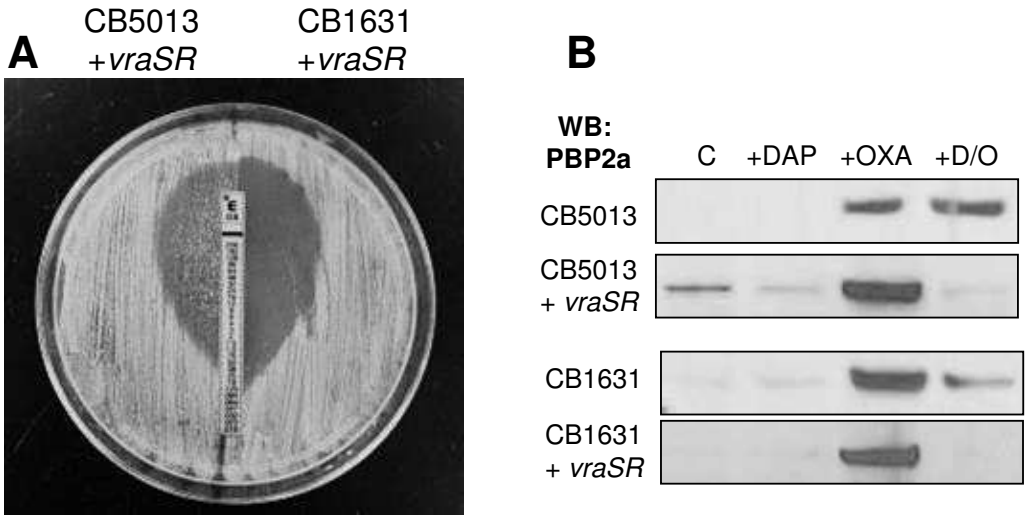

Fig 8. **VraSR and DAP-mediated see-saw effect.** (**A)** CB5013+*vraSR* and CB1631+*vraSR* strains were grown O/N after which the adjusted inoculum was plated onto MH agar and OXA Etest strips were placed on the plates, and incubated at 37°C for 24 h. (**B)** western blot analysis of PBP2a present in cell membrane extracts collected under the indicated conditions in DAPS CB5013 and CB1631, and their corresponding +vraSR counterparts (CB5013+*vraSR* and CB1631+*vraSR,* respectively).

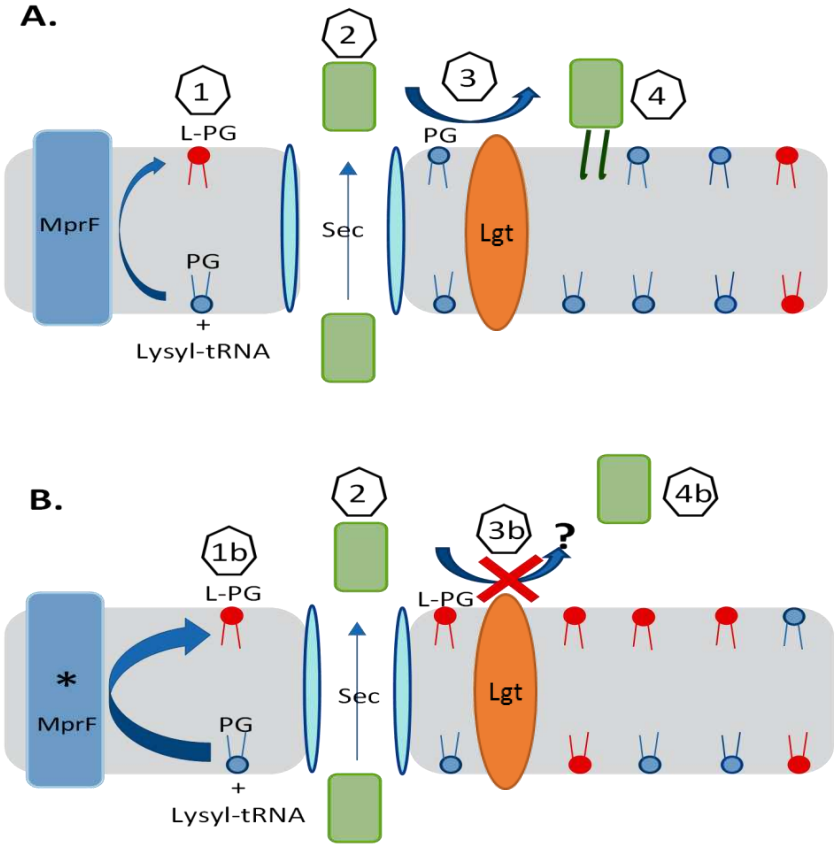

Fig 9. Proposed model of MprF (A) or mutated MprF* (B) affecting lipoprotein PrsA anchorage. 1. MprF uses cytosolic lysyl tRNA to convert phosphatidyl glycerol (PG) to lysyl phosphatidyl glycerol (L-PG). **1b.** Enhanced transferase and/or flippase activity of mutated MprF increases the proportion of L-PG compared to PG in the outer membraned leaflet. **2.** Prelipoprotein PrsA is secreted probably through Sec pathway. **3.** PG is used by Lgt enzyme to lipid modify PrsA lipobox cysteine. **3b.** Inhibition of Lgt-mediated acyl transfer to PrsA due to increased L-PG/reduced PG amounts in the outer membrane leaflet. **4.** Lipidated membrane-anchored PrsA will help post-translational maturation of PBP2A. **4b.** Failure to produce lipidated membrane-anchored PrsA.